Incorporating Vascular Structure Into Electric Volume Conduction Models of the Cochlea

Paul Wong, Qing Li
School of AMME, Faculty of Engineering and IT
The University of Sydney
Sydney, Australia

Paul Carter
Implants Development
Cochlear Limited
Sydney, Australia

***Abstract*—Volume conduction models (VCMs) of the cochlea have been used to investigate its response to electrical stimulation. However, existing models have not accounted for the presence of blood vessels, despite the relatively low resistivity of blood and the pervasiveness of the vascular network. The finite element model developed in this paper represents a first step towards a vascularized VCM of the cochlea. The results show that the inclusion of blood vessels makes localized differences to the current distribution, and that these differences are amplified when fibrous scar tissue and anisotropic nerve tissue are also modeled. Current densities and electric fields in the spiral ganglion are also affected, though the differences are not expected to have a major impact on activation thresholds. As predicted, larger vessels have a greater influence on the end result and should be considered in future modeling efforts.**

Keywords-Cochlear implants; finite element methods; bioimpedance

I. INTRODUCTION

The electrophysiology of the cochlea has been studied extensively, but since the inner ear is inaccessible during life the available techniques for carrying out these studies have been fairly limited. In early investigations by von Békésy [1], bulk impedance measurements were obtained experimentally from both anaesthetized and deceased guinea pigs. He created an equivalent electric circuit, now termed a lumped-element model (LEM), to help explain his findings. Others followed with their own measurements and models, leading to a variety of different circuit representations [2–7]. Despite their popularity, a major shortcoming of LEMs was that they completely neglected the three-dimensional spatial structure of the cochlea. Advances in computing technology have since enabled the use of sophisticated numerical solution methods, which have in turn made it feasible to solve the volume conduction problem directly. Volume conduction models (VCMs) from several different research groups [8–13] have yielded some useful insights over the years.

Unfortunately, VCMs have carried over legacy assumptions that were originally made due to limitations inherent to LEMs. Specifically, bulk measurements only provide the effective impedance between two points in a region, not the actual route taken by injected current [8]. The pioneering models by both von Békésy [1] and Girzon [8] deduced that the nervous system and vasculature were major grounding pathways from the cochlea to the rest of the body. Von Békésy's LEM combined the nervous and vascular pathways into a single grounding resistance since his bulk measurements did not reveal the contribution from each tissue type. Likewise, Girzon did not model blood vessels in his VCM, and suggested that they are "probably represented adequately…by lumping the nerve tissue and blood vessels together" [8]. He went on to justify their exclusion by noting that they occupied a smaller volume than neural tissue. Despite Girzon's calls for further investigation of the vascular pathways, subsequent models have continued to neglect the cochlear vasculature on the basis of these assumptions. Only one model in the literature distinctly accounts for intracochlear blood vessels – a simple LEM by Johnstone *et al.* [2].

The total resistance through a block of material does not, however, depend on its total volume, but rather its resistivity and the length and breadth of the path through it. The resistivity of blood is substantially lower than that of nervous tissue (cf. Table 1), as well as most other cochlear tissues. In addition, Axelsson [14] showed that the vessel network in the cochlea is pervasive. According to his account, the human cochlea is supplied solely by a branch of the anterior inferior cerebellar artery called the labyrinthine artery, which follows the auditory nerve through the internal acoustic meatus and splits into the anterior vestibular artery, the vestibulo-cochlear artery and the spiral modiolar artery. Radiating arterioles regularly branch off the spiral modiolar artery to feed convoluted capillary beds in the modiolus, the spiral lamina and the external wall. Collecting venules form as the capillaries

TABLE I. MATERIAL TYPES AND RESISTIVITIES

Material	Resistivity (Ω.m)
Bone	6.41
Nerve (axial)	3
(transverse)	15
Blood	1.5
Perilymph	0.7
Endolymph	0.6
Organ of Corti	83.333
Basilar membrane	80
Reissner's membrane	10,203.9
Spiral ligament	0.6
Stria vascularis	188.685
Fibrous tissue	6.27
Silicone	10,000,000
Platinum	0.001

978-1-4673-1666-8/12/$31.00 ©2012 IEEE

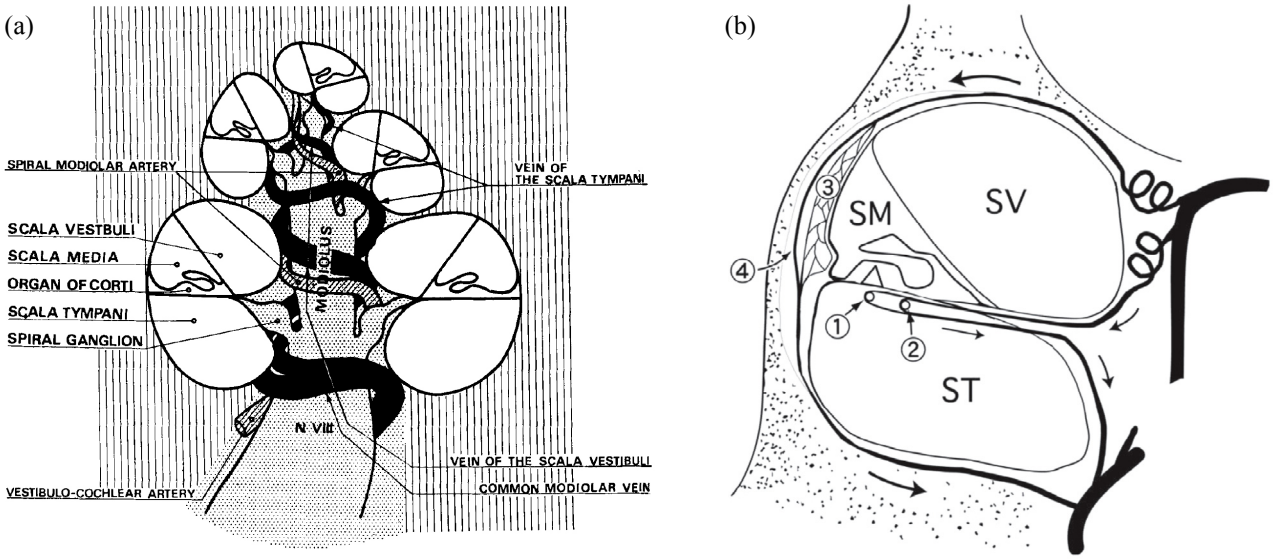

Figure 1. Schematics of (a) the major modiolar blood vessels by Axelsson [14]; and (b) smaller vessels in one turn of the cochlea by Nakashima [15].

recombine and drain into the veins of the scala vestibuli and scala tympani, which in turn merge into the vein of the cochlear aqueduct and leave the cochlea. Reissner's membrane and some parts of the organ of Corti are avascular. The large modiolar vessels and some of the smaller cross-sectional vessels are illustrated schematically in Fig. 1.

Recent models of other parts of the body have demonstrated differences in calculated outputs due to the presence of blood vessels. Kuang *et al.* [16] described impedance changes in the thorax via a mathematical model, and a study by Bishop *et al.* [17] showed that fine anatomical structures such as blood vessels have an impact in VCMs of the heart. It stands to reason that vessels through the cochlea might also have a similar effect. Considering all of the above, the dismissal of blood vessels from VCMs of the cochlea may be unwarranted.

A low resistance vascular pathway is of particular interest in the context of cochlear implants (CIs). These auditory prostheses use electrical stimulation to restore the perception of hearing in individuals with profound hearing loss. Modern CIs operate using a monopolar stimulation technique, with current flowing from the intracochlear stimulating electrode to a distant return electrode located just under the scalp. The blood vessel network along this return path is also pervasive, and early work by Tran *et al.* [18] has indicated that a preferential pathway may pass near the major cranial vessels. A vascularized VCM of the cochlea could tie in with this whole-head model. If this preferential pathway exists, it is likely to direct current away from the auditory nerve and change the extent of neural firing that is predicted by the VCM.

This paper documents a preliminary study on incorporating the blood vessels of the cochlea into a three-dimensional (3D) finite element (FE) volume conduction model. It aims to quantify the effects of blood vessels on current flow, thereby furthering our understanding of the cochlea's electric response and providing a guideline for incorporating such tissue types into future VCMs.

II. MODELLING

A. Anatomical Data

One reason for the absence of vascularized VCMs may be the lack of appropriate image data from which to reconstruct the anatomical geometry. Currently available data sets were of insufficient resolution and/or clarity for identifying and segmenting the cochlear vessels, so a compound approach was adopted for this early work.

A single histological slice of the human cochlea [19] measuring 709×1091 pixels was used to build the model. Tissue types from existing models were easily identified, while the areas representing blood vessels were visible but not completely clear. Therefore, a new protocol was developed to image the cochlear vessels *in situ*. Anaesthetized guinea pigs were perfused with Microfil (Flow Tech, Inc.), a lead-based contrast agent designed for vascular imaging. The cochleae were removed from the guinea pigs, decalcified and scanned with micro-CT. Some differences exist between the guinea pig cochlea and the human cochlea, for instance a single versus a double venous drainage system, but for the most part the structures are comparable. The locations of blood vessels in the histological slice were determined by referring to these new images and Axelsson's account [14].

B. Electrical Data

Impedances for cochlear tissues have been shown to be predominantly resistive up to frequencies of 12.5 kHz [20]. To allow for comparison with existing models, resistivity data that could be obtained from published work [8–13] was used where available. For blood, a survey of conductivity values revealed wide variations depending on such factors as temperature, haematocrit and flow velocity [21–23]. As such, an often referenced common value [24] was used.

The values for each tissue type used in this study can be found in Table 1.

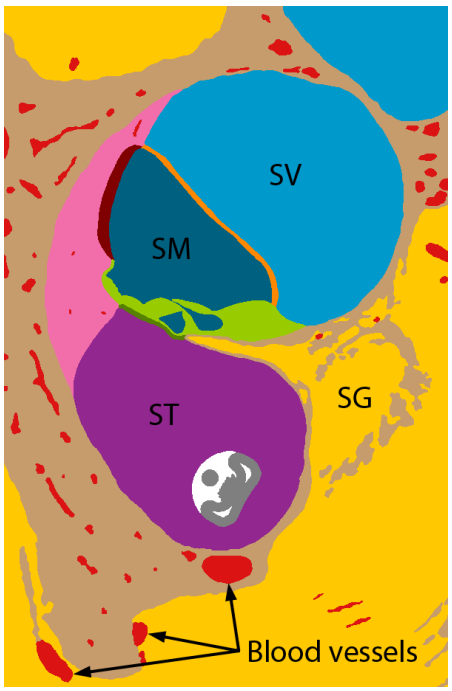

Figure 2. The pre-processed image with materials separated by colour. Regions in red denote blood vessels. The scala vestibuli (SV), scala media (SM), scala tympani (ST) and spiral ganglion (SG) are as labelled. Note also the intracochlear electrode array in the bottom of the scala tympani.

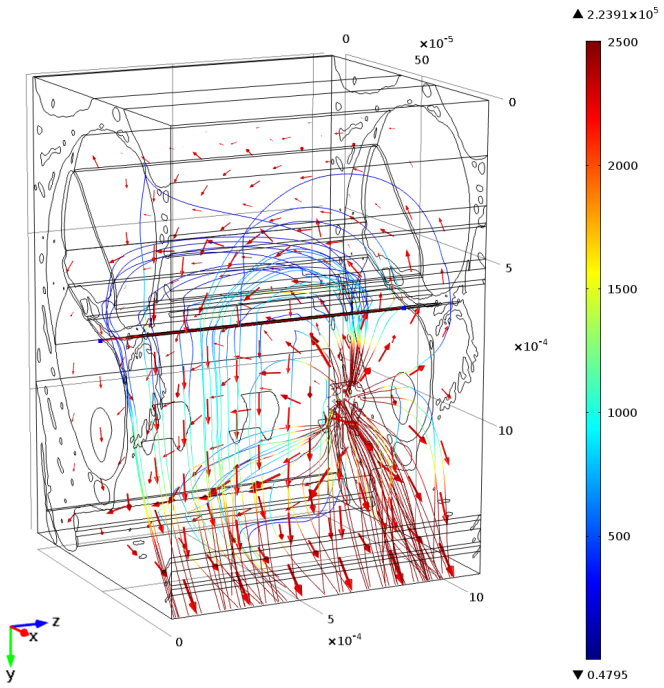

Figure 3. Streamline and vector combination plot of the B+BSN scenario. Streamlines indicate the trajectories from 80 equally distributed points on the electrode surface to ground, with color representing local current density. The vectors through the VST and surrounding bone indicate an increase in longitudinal current shunting via the blood vessels compared with the base case scenario.

C. *Image Processing*

The histological slice was pre-processed in Adobe Photoshop. Image contrast was enhanced using the Auto Tone functionality. Reissner's membrane was further enhanced using Gamma Correction since it was particularly hard to distinguish. Each tissue type of interest was then manually selected using the Lasso Tool, with feathering and anti-aliasing disabled to ensure accurate binarization. Each selection was filled with its own distinct solid color. A Cochlear CI422 electrode cross-section was added into the scala tympani at a position and orientation in line with images from a sectioned implanted cochlea (courtesy Cochlear Limited). The final pre-processed image can be seen in Fig. 2.

D. *Segmentation and Mesh Generation*

Segmentation and meshing were both performed in Simpleware ScanIP. A total of 22 pre-processed images were imported to create an extruded linear model containing three electrode contacts. The images were resampled to improve performance. A mask for each material type was then created using threshold segmentation. The vascular structures passing through bone, nerve and the spiral ligament were separated into three different domains to enable variation of material properties for the upcoming sensitivity analysis. For similar reasons, the scala tympani containing the implanted electrode array was also treated as a separate domain from the other perilymphatic chambers. Smoothing and morphological filters were applied to selected masks, taking care to patch any resultant gaps. All masks were then used to construct a FE model using the +FE Free meshing algorithm. The meshing parameters were tweaked over several iterations in order to optimize the quality of the mesh.

In terms of hardware, a custom built desktop computer with an Intel Core i7 3930K CPU and 64 GB of RAM was used. ScanIP took approximately 1 hour and 40 minutes to generate the final mesh, during which it reported a peak working set of about 15 GB. The mesh was then exported to COMSOL Multiphysics and consisted of 10,505,119 tetrahedral elements with 1,877,712 degrees of freedom.

E. *Analysis*

The electrical properties in Table 1 were assigned to each corresponding domain. Three factors were investigated: the presence of blood vessels, the formation of scar tissue, and nerve tissue anisotropy. The absence of all three was taken as the base case (B). Blood vessels were modeled by changing the resistivity of the vessel domains from that of the surrounding tissue to blood (B+B). Scar tissue was modeled by changing the resistivity of the implanted scala tympani from perilymph to fibrous tissue (B+BS), representing an extreme case where the entire chamber is filled with scar tissue. Nerve tissue anisotropy was modeled by changing its resistivity in the z-direction (i.e. along the scala, see Fig. 3) from the axial value to the transverse value (B+BSN), as it was assumed that nerve fibers run primarily in the radial direction, parallel to the xy-plane. The latter two cases were of interest because current shunting along the scala has been observed both experimentally and in existing models [25].

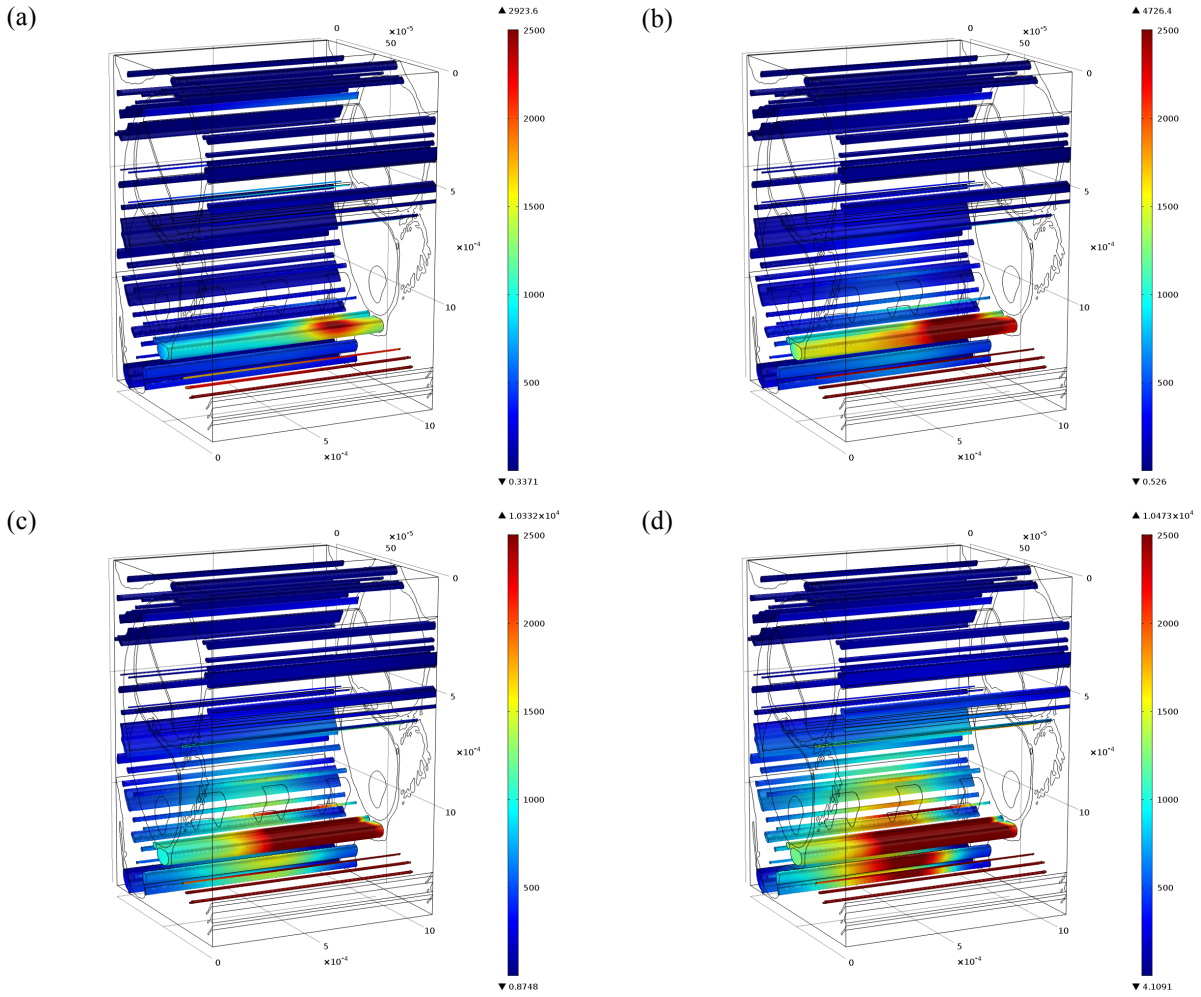

Figure 4. Current density contours of the blood vessel domains for the four scenarios: (a) B, (b) B+B, (c) B+BS, (d) B+BSN.

Regarding stimulation loads, a 1 mA terminal was applied on the interior surface of the far right platinum electrode. The model was grounded along the bottom edge corresponding to the modiolus to maintain consistency with observations and existing models that acknowledge the auditory nerve as the main grounding pathway. All other surfaces remained insulated.

During processing, all 12 CPU threads were active and the working set peaked at about 17 GB. Each simulation run took roughly 5 minutes and 30 seconds to complete.

III. Results

Fig. 3 shows the overall current paths in the B+BSN scenario. Current from the main electrode surface tends to travel directly toward the modiolus, while current from the lateral surfaces follows longer alternative paths and appear to be the main contributor to current spread. Of particular interest though is that the vectors through the vein of the scala tympani (VST) increase in magnitude and point in a more longitudinal direction compared to the base case, suggesting that more current is shunted along the cochlea relative to a non-vascularized model.

This view is reinforced by the current density contours in Fig. 4. When blood is added to the base case, there is a marked increase in current density in the blood vessels. The impact is largely localized to regions near the stimulating electrode and is most noticeable in the VST, though other vessels are also affected. Scar tissue formation amplifies this effect by cutting off the highly conductive perilymphatic pathway through the scala tympani. Similarly, anisotropic nerve tissue funnels even more current through the vascular network. Compared to the base case, the average current density along the VST increased by 181%, 273% and 314% in the B+B, B+BS, and B+BSN scenarios respectively. These results are consistent with the prediction that vessels provide a low impedance path between the source and the sink, and suggest that the vasculature may form a preferential exit pathway from the implanted cochlea.

The current density and electric field distributions in the spiral ganglion were also of interest since it is considered the site of neuronal stimulation in implanted individuals [26]. Plots of both quantities along the center of the spiral ganglion are shown in Fig. 5. As expected, the distributions are asymmetric, with both quantities showing peaks roughly aligned with the stimulating electrode. When blood is modeled, current densities fall by an average of 3.27% and 4.27% in the B+B and B+BSN

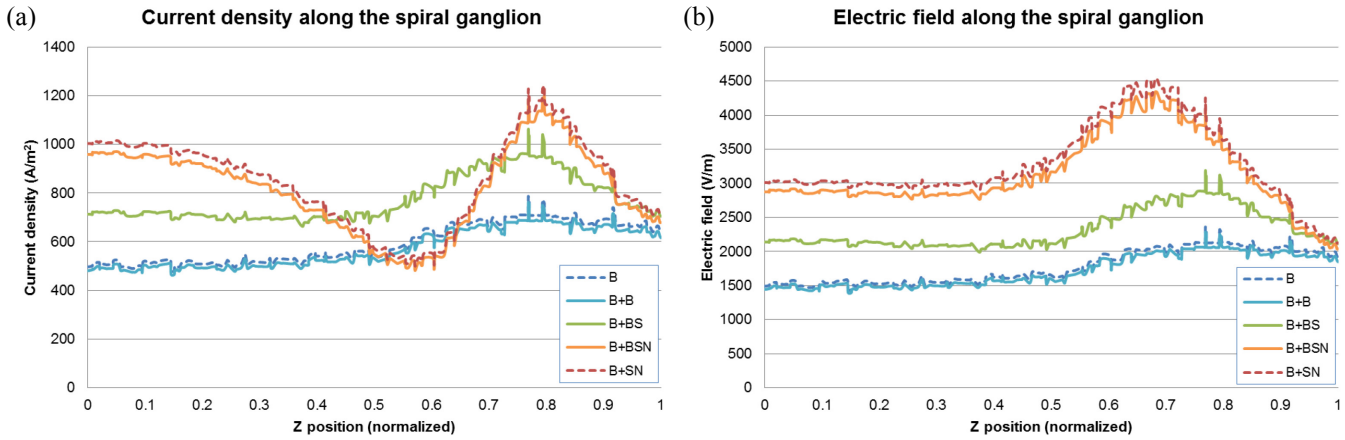

Figure 5. Comparison of (a) current density and (b) electric field along the spiral ganglion. The dotted lines represent non-vascularized scenarios.

cases respectively compared with their non-vascularized counterparts, providing further evidence that the vessel network redirects injected current away from the modiolus. Conversely, scar tissue increases current flow in the spiral ganglion by a significantly higher margin. When anisotropic nerve tissue is also modeled, the peak becomes higher and more focused. Current density reaches a minimum below that of the B+B scenario before increasing at points further from the stimulating electrode. This increase arises from two mechanisms: the high transverse resistivity of nerve tissue directs current into the scala vestibuli; the insulating boundary condition on the outer surfaces of the model then force the shunted current to return to ground by crossing back through the spiral ganglion (cf. Fig 3). An extended model could be expected to show a monotonic decrease away from the peak.

The electric field patterns show very similar trends. Magnitude peaks in the vicinity of the stimulating electrode and stabilizes at distance. Average field strength falls by 3.27% and 4.63% in the B+B and B+BSN cases respectively, again compared with their non-vascularized counterparts. Scar tissue increases the field by a larger margin, and nerve tissue anisotropy accentuates the peak. The gradient of the electric field (i.e. the second derivative of voltage) is also of interest because basic nerve fiber activation models cite it as the trigger for action potentials [27]. In this respect, the fields in Fig. 5 decrease with the addition of blood, so the gradient differences, which are proportional to the field difference, are also 3.27% and 4.63% for the B+B and B+BSN cases respectively. Nerve firing in the spiral ganglion is therefore unlikely to be significantly affected by the presence of blood vessels according to this model.

IV. Discussion

The model presented in this paper is a first pass at including the intracochlear vessels in a VCM. Some of the predictions are consistent with previous studies, for instance, the longitudinal current spread, a peak in electric field at the stimulating electrode, and the prevention of lateral current spread due to scar tissue formation. Other predictions, such as current paths and current densities, differ slightly from existing work available in the literature.

Some simplifications were made in the construction of this model that may affect the accuracy of these results. First and foremost, the geometry is not entirely realistic. Cross-sectional detail was captured well by the use of a histological slice, but the simple extrusion used to recreate a small portion of the cochlear turn à la Finley [9] is problematic. Other models have shown that the true 3D shape of the cochlea is significant in determining its electric response [11–13]. The representation of cochlear vessels has also been simplified due to the extrusion process. In the true anatomy, vessels do not run perfectly parallel to the scala. There are also radiating arterioles and collecting venules which are not modeled, so the vessel network is underrepresented here. Regardless, it is clear that the larger vessels, like the VST, the vessels near the stimulating electrode, as well as those in the modiolus are likely to have a significant impact on the conduction patterns. As such, these vessels should be included in future VCMs.

Another assumption worth examining is the tissue resistivities. Some variation has been observed between models over time, and like the legacy assumption regarding blood vessels, many of these have been carried over from the days of bulk impedance measurements so they may be inaccurate. Tissue properties are arguably second to the geometry in terms of importance to model accuracy, but there have been few efforts focused on that area to date. With regards to this model in particular, the anisotropy of nerve tissue was only partially accounted for, so its effect may be even more pronounced in a more sophisticated model that includes true fiber directions. Furthermore, blood vessel walls were not modeled. Edgerton measured them to be roughly four times more resistive than blood [28], putting them at a similar level to bone tissue. Since the walls of intracochlear vessels are thin, they are not expected to make a large difference within the cochlea, but it may be that current enters them easily and become trapped by the thicker walls of larger vessels upon exiting into the head. Note that vessel walls would be difficult to segment and incorporate into a FE model due to their small dimensions.

A final assumption of this model that has been entrenched in existing VCMs is the boundary conditions. The grounding of the auditory nerve in the modiolus [8,13], while convenient and logical to a certain extent, does not accurately represent the physical reality in current monopolar stimulation setups

because the ground electrodes are actually quite far from the cochlea. The main alternative, which is to embed the entire model in bone tissue and ground the entire periphery [10,11], is also questionable. As indicated by the results of this study, the presence of numerous blood vessels running through the bone may provide low-impedance paths for current flow that are not accounted for in existing models. The boundary conditions imposed on the model will undoubtedly have a significant effect on both the current paths and electric fields, in turn affecting the number and location of activated nerve fibers. Therefore, a more holistic view that incorporates volume conduction through the vascularized cochlea as well as the whole head needs to be pursued.

V. CONCLUSION

A 3D finite element VCM of the vascularized cochlea was created to investigate the effect of blood vessels on electric conduction in the implanted cochlea. Despite its simplicity, there were notable differences between the vascularized model and the base case scenario (representing existing models available in the literature) in terms of both local and global current density and electric field distributions. These early results indicate that the presence of vessels directs some current away from the auditory nerve, and although the small difference calculated in this model is not likely to affect the activation of spiral ganglion cells, other factors (particularly the boundary conditions) may be playing a limiting role. Further refinements to the model are required in order to make more definitive statements. Future models should include at least the larger blood vessels and those in the modiolus, as these seem to have a larger impact on the end results.

ACKNOWLEDGMENTS

The author would like to thank Ian Curthoys from the School of Psychology, and Allan Jones and Christopher Wong from the Australian Centre for Microscopy & Microanalysis at The University of Sydney, for their continued efforts in preparing and imaging the guinea pig specimens.

The author would also like to thank Cochlear Limited for providing reference geometries and images for this study.

REFERENCES

[1] G. von Békésy, "The coarse pattern of the electrical resistance in the cochlea of the guinea pig (electroanatomy of the cochlea)," J. Acoust. Soc. Am., vol. 23, p. 18, 1951.

[2] B. M. Johnstone, J. R. Johnstone, and I. D. Pugsley, "Membrane resistance in endolymphatic walls of the first turn of the guinea-pig cochlea". J. Acoust. Soc. Am., vol. 40, pp. 1398–1404, 1966.

[3] D. Strelioff, "A computer simulation of the generation and distribution of cochlear potentials," J. Acoust. Soc. Am., vol. 54, p. 620, 1973.

[4] R. C. Black, G. M. Clark, Y. C. Tong, and J. F. Patrick, "Current distributions in cochlear stimulation," Ann. N. Y. Acad. Sci., vol. 405, pp. 137–145, 1983.

[5] M. F. Suesserman and F. A. Spelman, "Lumped-parameter model for in vivo cochlear stimulation," IEEE Trans. Biomed. Eng., vol. 40(3), pp. 237–245, 1993.

[6] G. A. S. Machado and C. Toumazou, "Analytical generation of parameters for in-vivo lumped-parameter models of implanted and normal cochleae," Engineering in Medicine and Biology Society, IEEE 17th Annual Conference, vol. 2, pp. 1607–1608, 1995.

[7] F. J. Vanpoucke, A. J. Zarowski, and S. A. Peeters, "Identification of the impedance model of an implanted cochlear prosthesis from intracochlear potential measurements," IEEE Trans. Biomed. Eng., vol. 51(12), pp. 2174–2183, 2004.

[8] G. Girzon, "Investigation of current flow in the inner ear during electrical stimulation of intracochlear electrodes," Master's thesis, Massachusetts Institute of Technology, Dept. of Electrical Engineering and Computer Science, 1987.

[9] C. C. Finley, B. S. Wilson, and M. W. White, "Models of neural responsiveness to electrical stimulation," Cochlear implants: models of the electrically stimulated ear, vol. 56, 1990.

[10] J. H. M. Frijns, R. K. Kalkman, F. J. Vanpoucke, J. S. Bongers, and J. J. Briaire, "Simultaneous and non-simultaneous dual electrode stimulation in cochlear implants: evidence for two neural response modalities," Acta Oto-Laryngol., vol. 129(4), pp. 433–439, 2009.

[11] T. Hanekom, "Three-dimensional spiraling finite element model of the electrically stimulated cochlea," Ear Hear., vol. 22(4), p. 300, 2001.

[12] C. T. M. Choi and C. H. Hsu, "Conditions for generating virtual channels in cochlear prosthesis systems," Ann. Biomed. Eng., vol. 37(3), pp. 614–624, 2009.

[13] D. M. Whiten, "Electro-anatomical models of the cochlear implant," PhD thesis, Massachusetts Institute of Technology, 2007.

[14] A. Axelsson, "The vascular anatomy of the cochlea in the guinea pig and in man," Acta Oto-laryngol., pp. 5–134, 1968.

[15] T. Nakashima, et al., "Disorders of cochlear blood flow," Brain Res. Rev., vol. 43(1), pp. 17–28, 2003.

[16] M. X. Kuang, et al., "Mechanism of the formation of thoracic impedance change," Ann. Biomed. Eng., vol. 38(3), pp. 1007–1016, 2010.

[17] M. J. Bishop, et al., "Development of an anatomically detailed MRI-derived rabbit ventricular model and assessment of its impact on simulations of electrophysiological function," Am. J. Physiol.: Heart Circ. Physiol., vol. 298, pp. H699–H718, 2010.

[18] P. Tran, Q. Li , and P. Carter, "Finite element modelling of current flow from cochlear implant stimulation," Proceedings of the IASTED International Conference on Modelling, Simulation, and Identification, Pittsburgh, USA, November 2011.

[19] H. J. ten Donkelaar, M. Lammens, and A. Hori, Clinical Neuroembryology: Development and developmental disorders of the human central nervous system. Heidelberg: Springer, 2006.

[20] F. A. Spelman, B. M. Clopton, and B. E. Pfingst, "Tissue impedance and current flow in the implanted ear: Implications for the cochlear prosthesis," Ann. Otol., Rhinol., Laryngol., Suppl., vol. 98, p. 3, 1982.

[21] F. Jaspard and M. Nadi, "Dielectric properties of blood: an investigation of temperature dependence," Physiol. Meas., vol. 23, p. 547, 2002.

[22] F. Jaspard, M. Nadi, and A. Rouane, "Dielectric properties of blood: an investigation of haematocrit dependence," Physiol. Meas., vol. 24, p. 137, 2003.

[23] A. E. Hoetink, T. J. C. Faes, K. R. Visser, and R. M. Heethaar, "On the flow dependency of the electrical conductivity of blood," IEEE Trans. Biomed. Eng., vol. 51(7), pp. 1251–1261, 2004.

[24] S. N. Mohapatra, K. L. Costeloe, and D. W. Hill, "Blood resistivity and its implications for the calculation of cardiac output by the thoracic electrical impedance technique," Intensive Care Med., vol. 3(2), pp. 63–67, 1977.

[25] A. G. Micco and C. P. Richter, "Tissue resistivities determine the current flow in the cochlea," Curr. Opin. Otolaryngol. Head Neck Surg., vol. 14(5), p. 352, 2006.

[26] J. H. M. Frijns, J. J. Briaire, and R. Schoonhoven, "Integrated use of volume conduction and neural models to simulate the response to cochlear implants," Simulat. Pract. and Theor., vol. 8, pp. 75–97, 2000.

[27] A. G. Brown, Nerve cells and nervous systems: an introduction to neuroscience. Springer Verlag, 2001.

[28] R. H. Edgerton, "Radial conductivity of arterial walls," Med. Biol. Eng. Comput., vol. 13(4), pp. 531–534, 1975